

Z' resonance and associated Zh production at future Higgs boson factory: ILC and CLIC

A. Gutiérrez-Rodríguez^{*1} and M. A. Hernández-Ruíz^{†2}

¹*Facultad de Física, Universidad Autónoma de Zacatecas
Apartado Postal C-580, 98060 Zacatecas, México.*

²*Unidad Académica de Ciencias Químicas, Universidad Autónoma de Zacatecas
Apartado Postal C-585, 98060 Zacatecas, México.*

(Dated: March 5, 2022)

Abstract

We study the prospects of the B-L model with an additional Z' boson to be a Higgs boson factory at high-energy and high-luminosity linear electron positron colliders, such as the ILC and CLIC, through the Higgs-strahlung process $e^+e^- \rightarrow (Z, Z') \rightarrow Zh$, including both the resonant and non-resonant effects. We evaluate the total cross section of Zh and we calculate the total number of events for integrated luminosities of 500-2000 fb^{-1} and center of mass energies between 500 and 3000 GeV . We find that the total number of expected Zh events can reach 10^6 , which is a very optimistic scenario and it would be possible to perform precision measurements for both the Z' and Higgs boson in future high-energy e^+e^- colliders experiments.

PACS numbers: 12.60.-i, 12.15.Mm, 13.66.Fg

Keywords: Models beyond the standard model, neutral currents, gauge and Higgs boson production in e^+e^- interactions.

* alexgu@fisica.uaz.edu.mx

† mahernan@uaz.edu.mx

I. INTRODUCTION

The discovery of a light scalar boson H of the ATLAS [1] and CMS [2] Collaborations at the Large Hadron Collider (LHC) compatible with a SM Higgs boson [3–7] and with mass around $M_h = 125 \pm 0.4(\text{stat.}) \pm 0.5(\text{syst.}) \text{ GeV}$ has opened a window to new sectors in the search for physics beyond the Standard Model (SM). The Higgs boson might be a portal leading to more profound physics models and even physics principles. Therefore, another Higgs factory besides the LHC, such as the International Linear Collider (ILC) [8–13] and the Compact Linear Collider (CLIC) [14–16] that can study in detail and can precisely determine the properties of the Higgs boson is another important future step in high-energy and high-luminosity physics exploration.

The existence of a heavy neutral (Z') vector boson is a feature of many extensions of the Standard Model. In particular, one (or more) additional $U(1)'$ gauge group provides one of the simplest extensions of the SM. Additional Z' gauge bosons appear in Grand Unified Theories (GUTs) [17], Superstring Theories [18], Left-Right Symmetric Models (LRSM) [19–21] and in other models such as models of composite gauge bosons [22]. In particular, it is possible to study some phenomenological features associated with this extra neutral gauge boson by considering a $B - L$ (baryon number minus lepton number) model.

The $B - L$ symmetry plays an important role in various physics scenarios beyond the SM: a) the gauge $U(1)_{B-L}$ symmetry group is contained in a GUT described by a $SO(10)$ group [23]. b) the scale of the $B - L$ symmetry breaking is related to the mass scale of the heavy right-handed Majorana neutrinos mass terms providing the well-known see-saw mechanism [24] to explain light left-handed neutrino mass. c) the $B - L$ symmetry and the scale of its breaking are tightly connected to the baryogenesis mechanism through leptogenesis [25].

The $B - L$ model [26, 27] is attractive due to its relatively simple theoretical structure, and the crucial test of the model is the detection of the new heavy neutral (Z') gauge boson. The analysis of precision electroweak measurements indicates that the new Z' gauge boson should be heavier than about 1.2 TeV [28]. On the other hand, recent bounds from the LHC indicate that the Z' gauge boson should be heavier than about 2 TeV [29, 30], while future LHC runs at $13\text{-}14 \text{ TeV}$ could increase the Z' mass bounds to higher values, or may be lucky and find evidence for its presence. Further studies of the Z' properties will require a new linear collider [31], which will also allow us to perform precision studies of the Higgs sector.

Detailed discussions on the $B - L$ model can be found in the literature [26, 32–35, 37–39].

The Higgs-strahlung [40–44] process $e^+e^- \rightarrow Zh$ is one of the main production mechanisms of the Higgs boson in the future linear e^+e^- colliders experiments, such as the ILC and CLIC. Therefore, after the discovery of the Higgs boson, detailed experimental and theoretical studies are necessary for checking its properties and dynamics [45–48]. It is possible to search for the Higgs boson in the framework of the B-L model, however the existence of a new gauge boson could also provide new Higgs particle production mechanisms, which could prove its non-standard origin. In this work, we analyze how the Z' gauge boson of the $U(1)_{B-L}$ model could be used as a factory of Higgs bosons.

Our aim in the present paper is to study the sensitivity of the Z' boson of the B-L model as a Higgs boson factory through the Higgs-strahlung process $e^+e^- \rightarrow (Z, Z') \rightarrow Zh$, including both the resonant and non-resonant effects at future high-energy and high-luminosity linear e^+e^- colliders, such as the International Linear Collider (ILC) [8] and the Compact Linear Collider (CLIC) [14]. We evaluate the total cross section of Zh and we calculate the total number of events for integrated luminosities of 500-2000 fb^{-1} and center-of-mass energies between 500 and 3000 GeV . We find that the total number of expected Zh events for the e^+e^- colliders is very promising and that it would be possible to perform precision measurements for both the Z' and Higgs boson in the future high-energy e^+e^- colliders experiments. In addition, we also studied the dependence of the Higgs signal strengths (μ) on the parameters g'_1 and θ_{B-L} of the $U(1)_{B-L}$ model for the Higgs-strahlung process $e^+e^- \rightarrow Zh$.

This paper is organized as follows. In Section II, we present the theoretical framework. In Section III, we present the decay widths of the Z' boson in the context of the B-L model. In Section IV, we present the calculation of the process $e^+e^- \rightarrow (Z, Z') \rightarrow Zh$, and finally, we present our results and conclusions in Section V.

II. THEORETICAL FRAMEWORK

We consider an $SU(2)_L \times U(1)_Y \times U(1)_{B-L}$ model consisting of one doublet Φ and one singlet χ and briefly describe the lagrangian including the scalar, fermion and gauge sector. The Lagrangian for the gauge sector is given by [36, 37, 49, 50]

$$\mathcal{L}_g = -\frac{1}{4}B_{\mu\nu}B^{\mu\nu} - \frac{1}{4}W_{\mu\nu}^a W^{a\mu\nu} - \frac{1}{4}Z'_{\mu\nu}Z'^{\mu\nu}, \quad (1)$$

where $W_{\mu\nu}^a$, $B_{\mu\nu}$ and $Z'_{\mu\nu}$ are the field strength tensors for $SU(2)_L$, $U(1)_Y$ and $U(1)_{B-L}$, respectively.

The Lagrangian for the scalar sector of the $SU(2)_L \times U(1)_Y \times U(1)_{B-L}$ model is

$$\mathcal{L}_s = (D^\mu\Phi)^\dagger(D_\mu\Phi) + (D^\mu\chi)^\dagger(D_\mu\chi) - V(\Phi, \chi), \quad (2)$$

where the potential term is [34],

$$V(\Phi, \chi) = m^2(\Phi^\dagger\Phi) + \mu^2|\chi|^2 + \lambda_1(\Phi^\dagger\Phi)^2 + \lambda_2|\chi|^4 + \lambda_3(\Phi^\dagger\Phi)|\chi|^2. \quad (3)$$

with Φ and χ as the complex scalar Higgs doublet and singlet fields, respectively. The covariant derivatives for the doublet and singlet are given by [32–34]

$$\begin{aligned} D^\mu\Phi &= \partial_\mu\Phi + i[gT^a W_\mu^a + g_1 Y B_\mu + g'_1 Y' B'_\mu]\Phi, \\ D^\mu\chi &= \partial_\mu\chi + i[g_1 Y B_\mu + g'_1 Y' B'_\mu]\chi, \end{aligned} \quad (4)$$

where the doublet and singlet scalars are

$$\Phi = \begin{pmatrix} G^\pm \\ \frac{v+\phi^0+iG_Z}{\sqrt{2}} \end{pmatrix}, \quad \chi = \left(\frac{v' + \phi'^0 + iz'}{\sqrt{2}} \right), \quad (5)$$

with G^\pm , G_Z and z' the Goldstone bosons of W^\pm , Z and Z' , respectively.

After spontaneous symmetry breaking the two scalar fields can be written as,

$$\Phi = \begin{pmatrix} 0 \\ \frac{v+\phi^0}{\sqrt{2}} \end{pmatrix}, \quad \chi = \frac{v' + \phi'^0}{\sqrt{2}}, \quad (6)$$

with v and v' real and positive. Minimization of Eq. (3) gives

$$\begin{aligned} m^2 + 2\lambda_1 v^2 + \lambda_3 v v'^2 &= 0, \\ \mu^2 + 4\lambda_2 v'^2 + \lambda_3 v^2 v' &= 0. \end{aligned} \quad (7)$$

To compute the scalar masses, we must expand the potential in Eq. (3) around the minima in Eq. (6). Using the minimization conditions, we have the following scalar mass matrix:

$$\mathcal{M} = \begin{pmatrix} \lambda_1 v^2 & \frac{\lambda_3 v v'}{2} \\ \frac{\lambda_3 v v'}{2} & \lambda_2 v'^2 \end{pmatrix} = \begin{pmatrix} \mathcal{M}_{11} & \mathcal{M}_{12} \\ \mathcal{M}_{21} & \mathcal{M}_{22} \end{pmatrix}. \quad (8)$$

The expressions for the scalar mass eigenvalues ($m_{H'} > m_h$) are

$$m_{H',h}^2 = \frac{(\mathcal{M}_{11} + \mathcal{M}_{22}) \pm \sqrt{(\mathcal{M}_{11} - \mathcal{M}_{22})^2 + 4\mathcal{M}_{12}^2}}{2}, \quad (9)$$

and the mass eigenstates are linear combinations of ϕ^0 and ϕ'^0 , and written as,

$$\begin{pmatrix} h \\ H' \end{pmatrix} = \begin{pmatrix} \cos \alpha & -\sin \alpha \\ \sin \alpha & \cos \alpha \end{pmatrix} \begin{pmatrix} \phi^0 \\ \phi'^0 \end{pmatrix}, \quad (10)$$

where h is the SM-like Higgs boson. The scalar mixing angle, α can be expressed as

$$\tan(2\alpha) = \frac{2\mathcal{M}_{12}}{\mathcal{M}_{11} - \mathcal{M}_{22}} = \frac{\lambda_3 v v'}{\lambda_1 v^2 - \lambda_2 v'^2}. \quad (11)$$

In the Lagrangian of the $SU(2)_L \times U(1)_Y \times U(1)_{B-L}$ model, the terms for the interactions between neutral gauge bosons Z, Z' and a pair of fermions of the SM can be written in the form [37, 38]

$$\mathcal{L}_{NC} = \frac{-ig}{\cos \theta_W} \sum_f \bar{f} \gamma^\mu \frac{1}{2} (g_V^f - g_A^f \gamma^5) f Z_\mu + \frac{-ig}{\cos \theta_W} \sum_f \bar{f} \gamma^\mu \frac{1}{2} (g_V^{\prime f} - g_A^{\prime f} \gamma^5) f Z'_\mu. \quad (12)$$

From this Lagrangian we determine the expressions for the new couplings of the Z, Z' bosons with the SM fermions, which are given by

$$\begin{aligned} g_V^f &= T_3^f \cos \theta_{B-L} - 2Q_f \sin^2 \theta_W \cos \theta_{B-L} + \frac{2g_1'}{g} \cos \theta_W \sin \theta_{B-L}, \\ g_A^f &= T_3^f \cos \theta_{B-L}, \end{aligned} \quad (13)$$

$$\begin{aligned} g_V^{\prime f} &= -T_3^f \sin \theta_{B-L} - 2Q_f \sin^2 \theta_W \sin \theta_{B-L} + \frac{2g_1'}{g} \cos \theta_W \cos \theta_{B-L}, \\ g_A^{\prime f} &= -T_3^f \sin \theta_{B-L}, \end{aligned} \quad (14)$$

where $g = e/\sin\theta_W$ and θ_{B-L} is the $Z - Z'$ mixing angle. The current bound on this parameter is $|\theta_{B-L}| \leq 10^{-3}$ [51]. In the decoupling limit, that is to say, when $g'_1 = 0$ and $\theta_{B-L} = 0$ the couplings of the SM are recovered.

III. THE DECAY WIDTHS OF Z' IN THE B-L MODEL

In this section we present the new decay widths of the Z' boson [28, 52–54] in the context of the B-L model which we need in the calculation of the cross section for the process $e^+e^- \rightarrow Zh$. The Z' partial decay widths involving vector bosons and the scalar boson are

$$\Gamma(Z' \rightarrow W^+W^-) = \frac{G_F M_W^2}{24\pi\sqrt{2}} \cos^2\theta_W \sin^2\theta_{B-L} M_{Z'} \left(\frac{M_{Z'}}{M_Z}\right)^4 \left(1 - 4\frac{M_W^2}{M_{Z'}^2}\right)^{1/3} \left[1 + 20\frac{M_W^2}{M_{Z'}^2} + 12\frac{M_W^4}{M_{Z'}^4}\right], \quad (15)$$

$$\Gamma(Z' \rightarrow Zh) = \frac{G_F M_Z^2 M_{Z'}}{24\pi\sqrt{2}} \sqrt{\lambda} \left[\lambda + 12\frac{M_Z^2}{M_{Z'}^2}\right] \left[f(\theta_{B-L}) \cos\alpha - g(\theta_{B-L}) \sin\alpha\right]^2, \quad (16)$$

where

$$\begin{aligned} \lambda\left(1, \frac{M_Z^2}{M_{Z'}^2}, \frac{M_h^2}{M_{Z'}^2}\right) &= 1 + \left(\frac{M_Z^2}{M_{Z'}^2}\right)^2 + \left(\frac{M_h^2}{M_{Z'}^2}\right)^2 - 2\left(\frac{M_Z^2}{M_{Z'}^2}\right) - 2\left(\frac{M_h^2}{M_{Z'}^2}\right) - 2\left(\frac{M_Z^2}{M_{Z'}^2}\right)\left(\frac{M_h^2}{M_{Z'}^2}\right), \\ f(\theta_{B-L}) &= \left(\frac{4M_Z^2}{v^2} - g_1'^2\right) \sin(2\theta_{B-L}) + \left(\frac{4g_1' M_Z}{v}\right) \cos(2\theta_{B-L}), \\ g(\theta_{B-L}) &= 4g_1'^2 \left(\frac{v'}{v}\right) \sin(2\theta_{B-L}). \end{aligned} \quad (17)$$

The vacuum expectation value v' is taken as $v' = 2TeV$, while $\alpha = \frac{\pi}{9}$ for the Higgs mixing parameter in correspondence with Refs. [1, 2, 36, 55]. In our analysis we take $v = 246GeV$ and constrain the other scale, v' , by the lower bounds imposed on the mass of the extra neutral gauge boson Z' . The mass of the Z' and of the heavy neutrinos depend on v' , and should be related to it, while the Higgs masses depend on the angle α , the value of which is completely arbitrary.

Finally, the decay width of the Z' boson to fermions is given by

$$\Gamma(Z' \rightarrow f\bar{f}) = \frac{2G_F}{3\pi\sqrt{2}} N_f M_Z^2 M_{Z'} \sqrt{1 - 4\left(\frac{M_f^2}{M_{Z'}^2}\right)} \left[(g_V^{f'})^2 \left\{ 1 + 2\left(\frac{M_f^2}{M_{Z'}^2}\right) \right\} + (g_A^{f'})^2 \left\{ 1 - 4\left(\frac{M_f^2}{M_{Z'}^2}\right) \right\} \right], \quad (18)$$

where N_f is the color factor ($N_f = 1$ for leptons, $N_f = 3$ for quarks) and the couplings g_V^f and g_A^f of the Z' boson with the SM fermions are given in Eq. (14).

IV. THE TOTAL CROSS SECTION OF $e^+e^- \rightarrow Zh$ IN THE B-L MODEL

In this section, we calculate the Higgs production cross section via the process $e^+e^- \rightarrow Zh$ in the context of the B-L model at future high-energy and high luminosity linear electron-positron colliders, such as the ILC and CLIC.

The Feynman diagrams contributing to the process $e^+e^- \rightarrow (Z, Z') \rightarrow Zh$ are shown in Fig. 1. The expressions for the total cross section of the Higgs-strahlung process for the different contributions, that is to say SM, B-L and SM-(B-L), respectively, can be written in the following compact form:

$$\begin{aligned}
\sigma(e^+e^- \rightarrow Zh)_{tot} &= \frac{G_F^2 M_Z^4}{24\pi} \left[(g_V^e)^2 + (g_A^e)^2 \right] \frac{s\sqrt{\lambda}[\lambda + 12M_Z^2/s]}{[(s - M_Z^2)^2 + M_Z^2\Gamma_Z^2]} \\
&+ \frac{G_F^2 M_Z^6}{384\pi} \left[(g_V^e)^2 + (g_A^e)^2 \right] \frac{s\sqrt{\lambda}[\lambda + 12M_{Z'}^2/s]}{M_{Z'}^2[(s - M_{Z'}^2)^2 + M_{Z'}^2\Gamma_{Z'}^2]} \\
&\times \left[f(\theta_{B-L}) \cos \alpha - g(\theta_{B-L}) \sin \alpha \right]^2 \\
&+ \frac{G_F^2 M_Z^6}{12\pi} \left[g_V^e g_V^e + g_A^e g_A^e \right] s\sqrt{\lambda} \left[\frac{1}{M_Z^2} (\lambda + 12M_Z^2/s) \right. \\
&+ \left. \frac{1}{M_{Z'}^2} (\lambda + 6(M_Z^2 - M_{Z'}^2)/s) + \frac{s\lambda}{8M_Z^2 M_{Z'}^2} (\lambda - 12M_Z^2/s) \right] \\
&\times \frac{[(s - M_Z^2)(s - M_{Z'}^2) + M_Z M_{Z'} \Gamma_Z \Gamma_{Z'}]}{[(s - M_Z^2)^2 + M_Z^2\Gamma_Z^2][(s - M_{Z'}^2)^2 + M_{Z'}^2\Gamma_{Z'}^2]} \\
&\times \left[f(\theta_{B-L}) \cos \alpha - g(\theta_{B-L}) \sin \alpha \right],
\end{aligned} \tag{19}$$

where

$$\lambda\left(1, \frac{M_Z^2}{s}, \frac{M_h^2}{s}\right) = \left(1 - \frac{M_Z^2}{s} - \frac{M_h^2}{s}\right)^2 - 4\frac{M_Z^2 M_h^2}{s^2}, \tag{20}$$

is the usual two-particle phase space function, while g_V^e , g_A^e , g_V^e , g_V^e , $f(\theta_{B-L})$ and $g(\theta_{B-L})$ are given in Eqs. (13), (14) and (17), respectively.

The expression given in the first term of Eq. (19) corresponds to the cross section with the exchange of the Z boson, while the second and third term come from the contributions

of the B-L model and of the interference, respectively. The SM expression for the cross section of the reaction $e^+e^- \rightarrow Zh$ can be obtained in the decoupling limit, that is to say, when $\theta_{B-L} = 0$ and $g'_1 = 0$, in this case the terms that depend on θ_{B-L} and g'_1 in (19) are zero and (19) is reduced to the expression given in Refs. [40, 44] for the standard model.

V. RESULTS AND CONCLUSIONS

A. Z' resonance and associated Zh production in the B-L model

In this section we evaluate the total cross section of the Higgs-strahlung process $e^+e^- \rightarrow (Z, Z') \rightarrow Zh$ in the context of the B-L model at next generation linear e^+e^- colliders such as the ILC and CLIC. Using the following values for numerical computation [51]: $\sin^2 \theta_W = 0.23126 \pm 0.00022$, $m_\tau = 1776.82 \pm 0.16 \text{ MeV}$, $m_b = 4.6 \pm 0.18 \text{ GeV}$, $m_t = 172 \pm 0.9 \text{ GeV}$, $M_W = 80.389 \pm 0.023 \text{ GeV}$, $M_Z = 91.1876 \pm 0.0021 \text{ GeV}$, $\Gamma_Z = 2.4952 \pm 0.0023 \text{ GeV}$, $M_h = 125 \pm 0.4$ and considering the most recent limit from LEP [56]:

$$\frac{M_{Z'}}{g'_1} \geq 7 \text{ TeV}, \quad (21)$$

in our numerical analysis, we obtain the total cross section $\sigma_{tot} = \sigma_{tot}(\sqrt{s}, M_{Z'}, g'_1)$. Thus, in our numerical computation, we will assume \sqrt{s} , $M_{Z'}$ and g'_1 as free parameters.

We do not consider the process $e^+e^- \rightarrow (Z, Z') \rightarrow ZH'$ [35] in our study since in major parts of the $U(1)_{B-L}$ model parameter space the higgs boson H' is quite heavy, and it is difficult to detect the process $e^+e^- \rightarrow ZH'$ when the relevant mechanism is $e^+e^- \rightarrow Zh$.

In Figs. 2-3 we present the total decay width of the Z' boson as a function of $M_{Z'}$ and the new $U(1)_{B-L}$ gauge coupling g'_1 , respectively, with the other parameters held fixed to three different values. From Fig. 2, we see that the total width of the Z' new gauge boson varies from a few to hundreds of GeV over a mass range of $500 \text{ GeV} \leq M_{Z'} \leq 3000 \text{ GeV}$, depending on the value of g'_1 . In the case of Fig. 3, a similar behavior is obtained in the range $0 \leq g'_1 \leq 1$ and depends on the value of $M_{Z'}$. The branching ratios versus Z' mass are given in Fig. 4 for different channels, that is to say, $BR(Z' \rightarrow f\bar{f})$, $BR(Z' \rightarrow Zh)$ and $BR(Z' \rightarrow W^+W^-)$, respectively. In this figure the $BR(Z' \rightarrow f\bar{f})$ is the sum of all BRs for the decays into fermions. We consider $\theta_{B-L} = 10^{-3}$, $g'_1 = 0.5$ and $500 \text{ GeV} \leq M_{Z'} \leq 3000 \text{ GeV}$.

To illustrate our results on the sensitivity of the Z' gauge boson of the B-L model as a

Higgs boson factory through the Higgs-strahlung process $e^+e^- \rightarrow (Z, Z') \rightarrow Zh$, including both the resonant and non-resonant effects at future high-energy and high luminosity linear e^+e^- colliders, such as the International Linear Collider (ILC) and the Compact Linear Collider (CLIC), we present the total cross section in Figs. 5-11.

In Fig. 5, we show the cross section $\sigma(e^+e^- \rightarrow Zh)$ for the different contributions as a function of the center-of-mass energy \sqrt{s} for $\theta_{B-L} = 10^{-3}$ and $g'_1 = 0.5$: the solid line correspond to the first term of Eq. (19), where in the $U(1)_{B-L}$ model the couplings g_V^f and g_A^f of the SM gauge boson Z to electrons receive contributions of the $U(1)_{B-L}$ model. The dashed line corresponds to the second term of Eq. (19), that is to say, is the pure B-L contribution. Finally, the dot-dashed line corresponds to the total cross section of the process $\sigma(e^+e^- \rightarrow Zh)$. From Figure 5, we can see that the cross section corresponding to the first term of the Eq. (19) decreases for large \sqrt{s} , whereas in the case of the cross section of the B-L model and the total cross section, respectively, these are increased for large values of the center-of-mass energy, reaching its maximum value at the resonance Z' boson, that is to say, $\sqrt{s} = 1500 \text{ GeV}$.

To see the effects of g'_1 , the free parameter of the B-L model on the process $e^+e^- \rightarrow (Z, Z') \rightarrow Zh$, we plot the relative correction $\delta\sigma/\sigma_{SM} = (\sigma_{tot} - \sigma_{SM})/\sigma_{SM}$ as a function of g'_1 for $M_{Z'} = 1500, 2000, 2500 \text{ GeV}$ and $\sqrt{s} = 1500, 2000, 2500 \text{ GeV}$ in Fig. 6. We can see that the relative correction reaches its maximum value between $0.1 \leq g'_1 \leq 2.5$ and remains almost constant as g'_1 increases.

The deviation of the cross section in our model from the SM one, $\delta\sigma/\sigma_{SM}$ is depicted in Fig. 7 as a function of $M_{Z'}$ for $\sqrt{s} = 1500 \text{ GeV}$ and three values of the g'_1 , new gauge coupling. Figure 7 shows that the relative correction is very sensitive to the gauge boson mass $M_{Z'}$ and for the gauge parameter $g'_1 = 0.2, 0.5, 0.8$, the peak of the total cross section emerges when the heavy gauge boson mass approximately equals $M_{Z'} = 1500, 1450, 1300 \text{ GeV}$, respectively. Thus, in a sizeable parameter region of the B-L model, the new heavy gauge boson Z' can produce a significant signal, which can be detected in future ILC and CLIC experiments.

We plot the total cross section of the reaction $e^+e^- \rightarrow Zh$ in Figure 8 as a function of the center of mass energy, \sqrt{s} for the values of the heavy gauge boson mass of $M_{Z'} = 1500, 2000, 2500 \text{ GeV}$ and $\theta_{B-L} = 10^{-3}$, $g'_1 = 0.2$, respectively. In this figure we observed that for $\sqrt{s} = M_{Z'}$, the resonant effect dominates the Higgs particle production. A similar

analysis was performed in Fig. 9, but in this case $\theta_{B-L} = 10^{-3}$ and $g'_1 = 0.5$. In both figures we show that the cross section is sensitive to the free parameters. Comparing Figs. 8 and 9, we observe that the height of the resonances is the same in both Figures, but the resonances are broader for larger g'_1 values, as the total width of the Z' boson increases with g'_1 , as it is shown in Fig.2.

Finally, in Fig. 10 we use the current values of $M_{Z'}$ and θ_{B-L} , as well as the value of the coupling constant g'_1 and center of mass energy \sqrt{s} of the collider to obtain contour plot 3D for the total cross section $\sigma_{tot} = \sigma_{tot}(\sqrt{s}, M_{Z'}, g'_1)$ of the process $e^+e^- \rightarrow Zh$ for $M_h = 125$ GeV and $\theta_{B-L} = 10^{-3}$. In this figure the resonance peaks for the boson Z' are evident for the entire range of allowed parameters of the $U(1)_{B-L}$ model.

TABLE I: Total production of ZH in the B-L model for $M_{Z'} = 1500, 2000, 2500$ GeV, $\mathcal{L} = 500, 1000, 2000$ fb $^{-1}$ (1st, 2nd, 3rd number, respectively, in the last 3 columns), $M_H = 125$ GeV, $g'_1 = 0.5$ and $\theta_{B-L} = 10^{-3}$.

$\mathcal{L} = 500, 1000, 2000$ fb $^{-1}$			
\sqrt{s}	$M_{Z'} = 1500$ GeV	$M_{Z'} = 2000$ GeV	$M_{Z'} = 2500$ GeV
500	85 131; 170 263; 340 526	44 609; 89 219; 178 439	34 747; 69 493; 138 987
1000	155 482; 310 964; 621 928	33 523; 67 047; 134 094	15 339; 30 678; 61 355
1500	1 234 000; 2 460 000; 4 930 000	75 192; 150 384; 300 768	18 004; 36 008; 72 016
2000	92 640; 185 282; 370 564	396 490; 792 980; 1 580 000	42 224; 84 449; 168 899
2500	20 276; 41 534; 83 069	52 144; 104 288; 208 577	163 538; 327 076; 654 151
3000	8 243; 16 487; 32 974	12 721; 25 442; 50 885	32 173; 64 346; 128 693

From Figs. 5-10, it is clear that the total cross section is sensitive to the value of the gauge boson mass $M_{Z'}$, center-of-mass energy \sqrt{s} and g'_1 , the new $U(1)_{B-L}$ gauge coupling, increases with the collider energy and reaching a maximum at the resonance of the Z' gauge boson. As an indicator of the order of magnitude, we present the Zh number of events in Table I, for several gauge boson masses, center-of-mass energies and g'_1 values and for a luminosity of $\mathcal{L} = 500, 1000, 2000$ fb $^{-1}$. We find that the possibility of observing the process $e^+e^- \rightarrow (Z, Z') \rightarrow Zh$ is very promising as shown in Table I, and it would be possible to perform precision measurements for both the Z' and Higgs boson in the future high-energy

linear e^+e^- colliders experiments. We observed in Table I that the cross section rises once the threshold for Zh production is reached, with the energy, until the Z' is produced resonantly at $\sqrt{s} = 1500, 2000$ and 2500 GeV , respectively, for the three cases. Afterwards it decreases with rising energy due to the Z and Z' propagators. Another promising production mode for studying the Z' boson and Higgs boson properties is $e^+e^- \rightarrow (\gamma, Z, Z') \rightarrow t\bar{t}h$ [57].

B. The Higgs signal strengths in the B-L model

Considering the Higgs boson decay channels, the Higgs signal strengths can be defined as

$$\mu_i = \frac{\sigma_{B-L} \times BR(h \rightarrow i)_{B-L}}{\sigma_{SM} \times BR(h \rightarrow i)_{SM}}, \quad (22)$$

where i denotes a possible final state of the Higgs boson decay, for example $b\bar{b}, W^+W^-, ZZ, gg$ and $\gamma\gamma$.

Fixing the Higgs boson mass to the measured value and considering the decays $h \rightarrow \gamma\gamma$, $h \rightarrow ZZ$, $h \rightarrow W^+W^-$, $h \rightarrow b\bar{b}$ and $h \rightarrow \tau^+\tau^-$, the ATLAS collaboration report [58] a signal strength of

$$\mu = 1.18_{-0.14}^{+0.15}. \quad (23)$$

The corresponding CMS collaboration result [59] is

$$\mu = 1.00 \pm 0.13. \quad (24)$$

Good consistency is found, for both experiments, across different decay modes and analyses categories related to different production modes.

In the B-L model, the modifications of the $hf\bar{f}$ (the SM fermions pair) and hVV ($V = W, Z$) couplings can give the extra contributions to the Higgs boson production processes. On the other hand, the loop-induced couplings, such as $h\gamma\gamma$ and hgg , could also be affected. Finally, beside the effects already seen in the Higgs-strahlung channel due to the couplings Eqs. (13), (14) and the functions given by Eq. (17), the exchange of s-channel heavy neutral gauge boson Z' also affected the production cross section. All effects can modify the signal strengths in a way that may be detectable at the future ILC/CLIC experiments.

In Fig. 11, we show the dependence of the Higgs signal strengths μ_i ($i = b\bar{b}, \gamma\gamma$) on the parameter g'_1 and θ_{B-L} for the Higgs-strahlung process $e^+e^- \rightarrow (Z, Z') \rightarrow Zh$, where (a) and (b) denote the Higgs signal strengths $\mu_{b\bar{b}}$ and $\mu_{\gamma\gamma}$, respectively.

Using $\theta_{B-L} = 10^3$ for the mixing angle and $M_h = 125 \text{ GeV}$ for the Higgs boson mass, the following bound on the signal strength is obtained:

$$\mu = 1.2^{+0.12}_{-0.16}, \quad (25)$$

which is consistent with that obtained for the ATLAS [58] and CMS [59] collaborations, Eqs. (23) and (24), respectively.

In conclusion, we consider the Z' heavy gauge boson of the B-L model as a Higgs boson factory, through the Higgs-strahlung process $e^+e^- \rightarrow (Z, Z') \rightarrow Zh$. We find that the future linear e^+e^- colliders experiments such as the ILC and CLIC could test the B-L model by measuring the cross section of the process $e^+e^- \rightarrow Zh$, and it would be possible to perform precision measurements of the Z' gauge boson and of the h Higgs boson, as well as of the parameters of the model θ_{B-L} and g'_1 , complementing other studies on the B-L model and on the Higgs-strahlung process. The SM expression for the cross section of the reaction $e^+e^- \rightarrow Zh$ can be obtained in the decoupling limit, that is to say, when $\theta_{B-L} = 0$ and $g'_1 = 0$, in this case the terms that depend on θ_{B-L} and g'_1 in (19) are zero and (19) is reduced to the expression given in Refs. [40, 44] for the standard model. We also studied the dependence of the Higgs signal strengths (μ) on the parameters g'_1 and θ_{B-L} of the $U(1)_{B-L}$ model for the Higgs-strahlung process $e^+e^- \rightarrow Zh$. We obtain a bound on (μ), which is consistent with that obtained for the ATLAS [58] and CMS [59] collaborations. In addition, the analytical and numerical results for the total cross section have never been reported in the literature before and could be of relevance for the scientific community.

Acknowledgments

We acknowledge support from CONACyT, SNI, PROMEP and PIFI (México).

-
- [1] G. Aad, *et al.*, [ATLAS Collaboration], *Phys. Lett.* **B716**, 1 (2012).
- [2] S. Chatrchyan, *et al.*, [CMS Collaboration], *Phys. Lett.* **B716**, 30 (2012) 30.
- [3] P. Higgs, *Phys. Lett.* **12**, 132 (1964).
- [4] Peter W. Higgs, *Phys. Rev. Lett.* **13**, 508 (1964).
- [5] Peter W. Higgs, *Phys. Rev.* **145**, 1156 (1966).
- [6] F. Englert and R. Brout, *Phys. Rev. Lett.* **13**, 321 (1964).
- [7] G. Guralnik, C. Hagen and T. Kibble, *Phys. Rev. Lett.* **13**, 585 (1964).
- [8] T. Abe, *et al.* [Am. LC Group], arXiv: hep-ex/0106057.
- [9] G. Aarons *et al.*, [ILC Collaboration], arXiv: 0709.1893 [hep-ph].
- [10] J. Brau, *et al.*, [ILC Collaboration], arXiv: 0712.1950 [physics.acc-ph].
- [11] H. Baer, T. Barklow, K. Fujii, *et al.*, arXiv:1306.6352 [hep-ph].
- [12] D. M. Asner, *et al.*, arXiv: 1310.0763 [hep-ph].
- [13] *Proceedings of the Workshop e^+e^- Collisions at 500 GeV: The Physics Potential*, Munich-AnneCy-Hamburg, ed. P. M. Zerwas, Reports DESY 92-123A, B; 93-123C.
- [14] E. Accomando, *et al.* [CLIC Physics Working Group Collaboration], arXiv: hep-ph/0412251, CERN-2004-005.
- [15] D. Dannheim, P. Lebrun, L. Linssen *et al.*, arXiv: 1208.1402 [hep-ex].
- [16] H. Abramowicz, *et al.*, [CLIC Detector and Physics Study Collaboration], arXiv: 1307.5288 [hep-ph].
- [17] R. W. Robinett, *Phys. Rev.* **D26**, 2388 (1982).
- [18] M. Green and J. Schwarz, *Phys. Lett.* **B149**, 117 (1984).
- [19] R. N. Mohapatra and P. B. Pal, in *Massive Neutrinos in Physics and Astrophysics*, (World Scientific, Singapore, 1991).
- [20] G. Senjanovic, *Nucl. Phys.* **B153**, 334 (1979).
- [21] G. Senjanovic and R. N. Mohapatra, *Phys. Rev.* **D12**, 1502 (1975).
- [22] U. Baur, *et al.*, *Phys. Rev.* **D35**, 297 (1987).
- [23] W. Buchmuller, C. Greub and P. Minkowski, *Phys. Lett.* **B267**, 395 (1991).
- [24] R.N. Mohapatra and G. Senjanovic, *Phys. Rev. Lett.* **44**, 912 (1980).
- [25] M. Fukugita and T. Yanagida, *Physics of Neutrinos and Applications to Astrophysics*,

- (Springer, Berlin, 2003).
- [26] L. Basso, *et al.*, *Phys. Rev.* **D80**, 055030 (2009).
 - [27] L. Basso, *et al.*, *JHEP* **0910**, 006 (2009).
 - [28] P. Langacker, *Rev. Mod. Phys.* **81**, 1199 (2009).
 - [29] ATLAS Collaboration, ATLAS-CONF-2013-017.
 - [30] CMS Collaboration, CMS-PAS-EXO-12-061.
 - [31] B. C. Allanach, *et al.*, arXiv:hep-ph/0403133.
 - [32] L. Basso, *et al.*, *Eur. Phys. J.* **C71**, 1613 (2011).
 - [33] L. Basso, S. Moretti and G. M. Pruna, *J. Phys. G: Nucl. Part. Phys.* **G39**, 025004 (2012).
 - [34] L. Basso, S. Moretti and G. M. Pruna, *Phys. Rev.* **D82**, 055018 (2010).
 - [35] L. Basso, *et al.*, *Eur. Phys. J.* **C71**, 1724 (2011).
 - [36] S. Khalil, *J. Phys. G: Nucl. Part. Phys.* **G35**, 055001 (2008).
 - [37] L. Basso, arXiv:1106.4462 [hep-hp].
 - [38] J. L. Díaz-Cruz, *et al.*, *J. Phys. G: Nucl. Part. Phys.* **G40**, 125002 (2013).
 - [39] Satoshi Iso, Nobuchica Ocada and Yuta Orikasa, *Phys. Rev.* **D80**, 115007 (2009).
 - [40] J. Ellis, M. K. Gaillard, and D. V. Nanopoulos, *Nucl. Phys.* **B106**, 292 (1976).
 - [41] B. L. Ioffe and V. A. Khoze, *Sov. J. Part. Nucl.* **9**, 50 (1978).
 - [42] B. W. Lee, C. Quigg, and H. B. Thacker, *Phys. Rev.* **D16**, 1519 (1977).
 - [43] J. D. Bjorken, *Proc. Summer Institute on Particle Physics*, SLAC Report 198 (1976).
 - [44] V. D. Barger, *et al.*, *Phys. Rev.* **D49**, 79 (1994).
 - [45] John Ellis, arXiv:1312.5672.
 - [46] S. Dawson, *et al.*, [Higgs working group], arXiv:1310.8361.
 - [47] M. Klute, *et al.*, arXiv:1301.1322.
 - [48] T. Behnke, *et al.*, arXiv:1306.6327.
 - [49] A. Ferroglia, A. Lorca and J. J. van der Bij, *Ann. Phys.* **16**, 563 (2007); and references therein.
 - [50] T. G. Rizzo, arXiv:hep-ph/0610104; and references therein.
 - [51] K. A. Olive, *et al.*, [Particle Data Group], *Chin. Phys.* **C38**, 090001 (2014).
 - [52] A. Leike, *Phys. Rep.* **317**, 143 (1999).
 - [53] R. W. Robinett and J. L. Rosner, *Phys. Rev.* **D25**, 3036 (1982).
 - [54] V. Barger and K. Whisnant, *Phys. Rev.* **D36**, 3429 (1987).
 - [55] Lorenzo Basso, Stefano Moretti, and Giovanni Marco Pruna, *Phys. Rev.* **D83**, 055014 (2011).

- [56] G. Cacciapaglia, C. Csaki, G. Marandella and A. Strumia, *Phys. Rev.* **D74**, 033011 (2006).
- [57] A. Gutiérrez-Rodríguez and M. A. Hernández-Ruíz, Work in progress.
- [58] ATLAS Collaboration, ATLAS-CONF-2015-007.
- [59] Vardan Khachatryan, *et al.*, [CMS Collaboration], *Eur. Phys. J.* **C75**, 212 (2015).

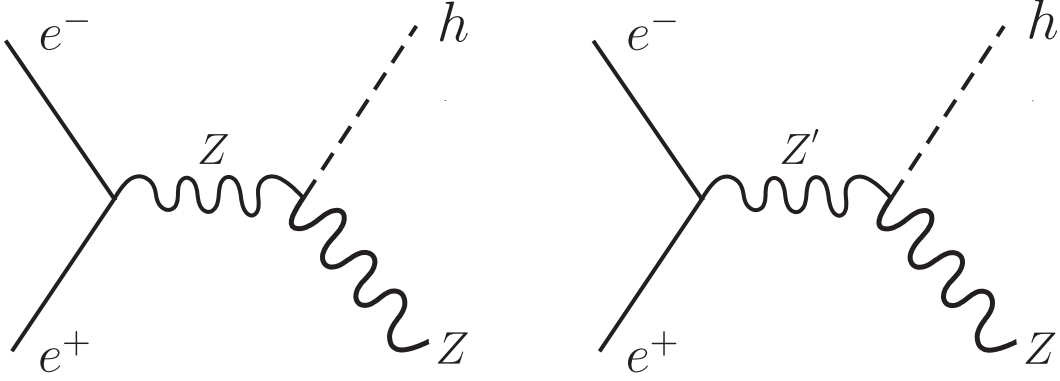


FIG. 1: Feynman diagram for the Higgs-strahlung process $e^+e^- \rightarrow Zh$ in the B-L model.

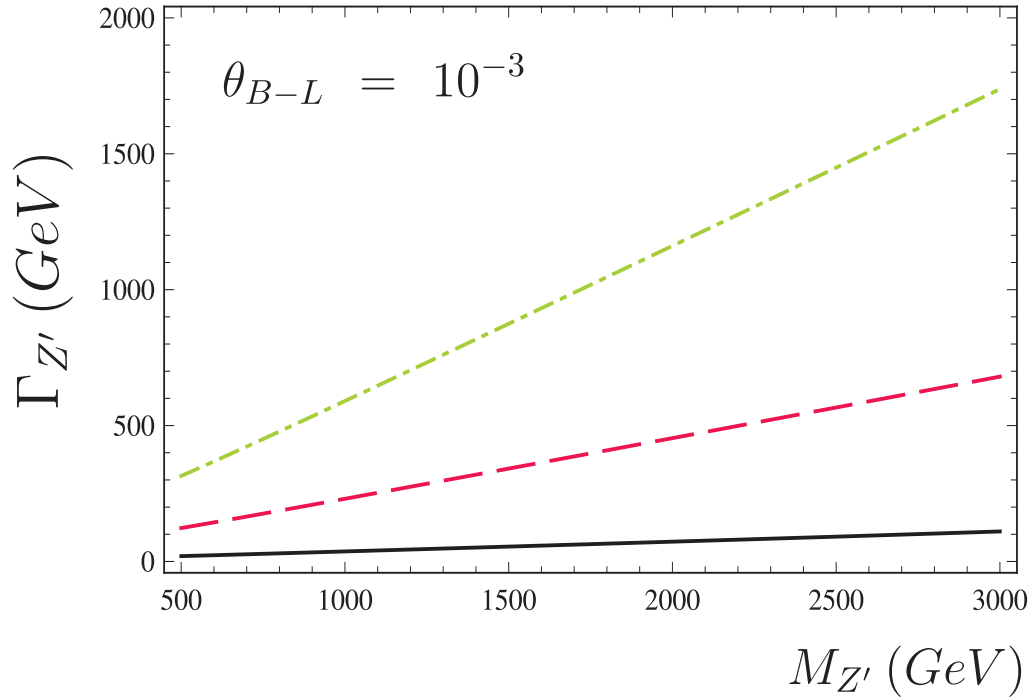


FIG. 2: Z' width as a function of $M_{Z'}$ for fixed values of g'_1 . Starting from the bottom, the curves are for $g'_1 = 0.2, 0.5, 0.8$, respectively.

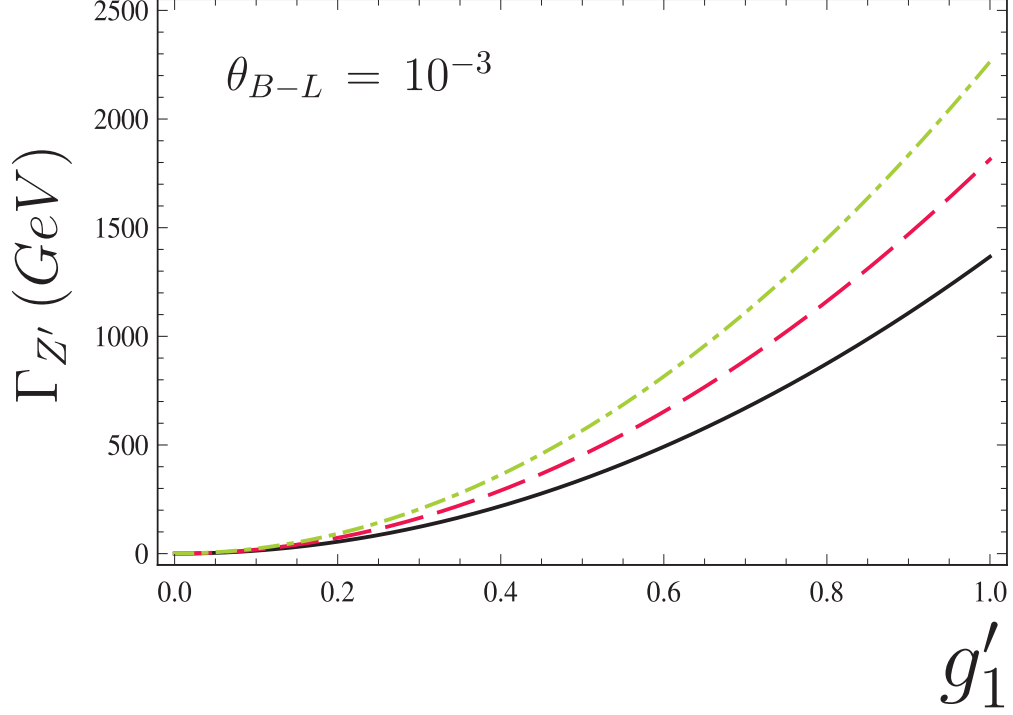


FIG. 3: Z' width as a function of g'_1 for fixed values of $M_{Z'}$. Starting from the bottom, the curves are for $M_{Z'} = 1500, 2000, 2500 \text{ GeV}$, respectively.

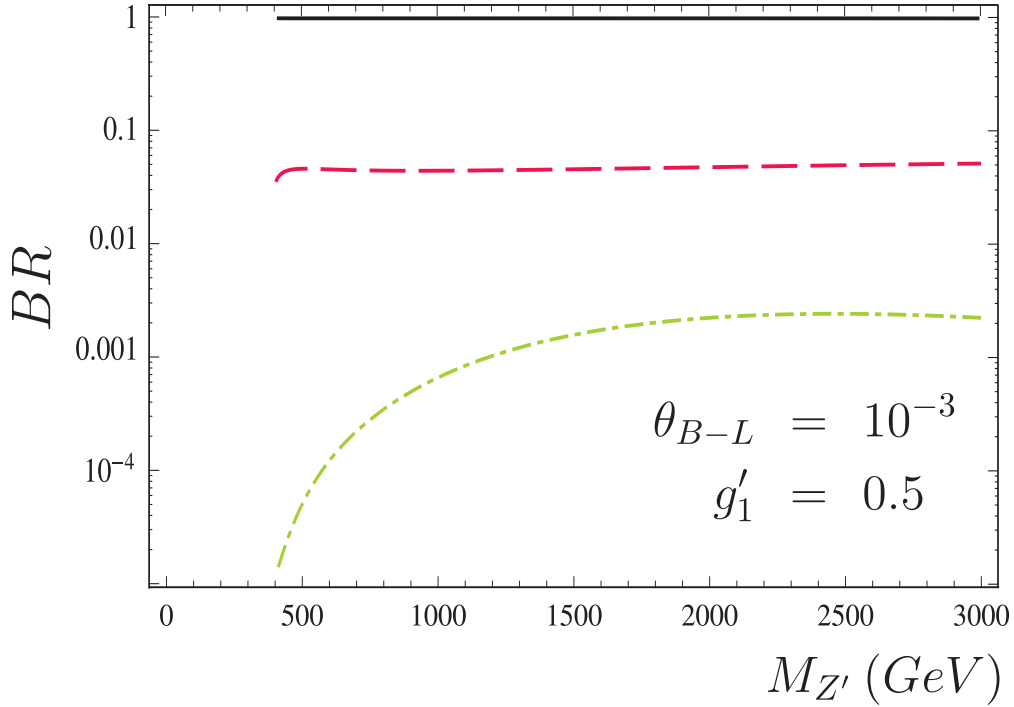


FIG. 4: Branching ratios as a function of $M_{Z'}$. Starting from the top, the curves are for the $BR(f\bar{f})$, $BR(Zh)$ and $BR(W^+W^-)$, respectively.

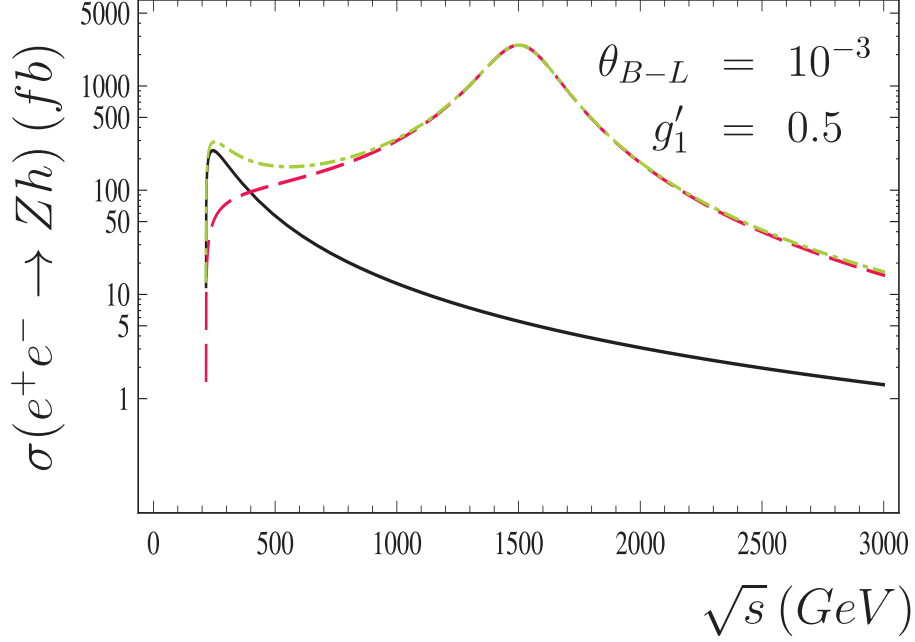


FIG. 5: The total cross sections of the production processes $e^+e^- \rightarrow Zh$ as a function of the collision energy for $M_{Z'} = 1500 \text{ GeV}$ and $M_h = 125 \text{ GeV}$. The curves are for the first term of Eq. (19) (solid line), second term of Eq. (19) (dashed line) and the dot-dashed line correspond to the total cross section of the process $\sigma(e^+e^- \rightarrow Zh)$, respectively.

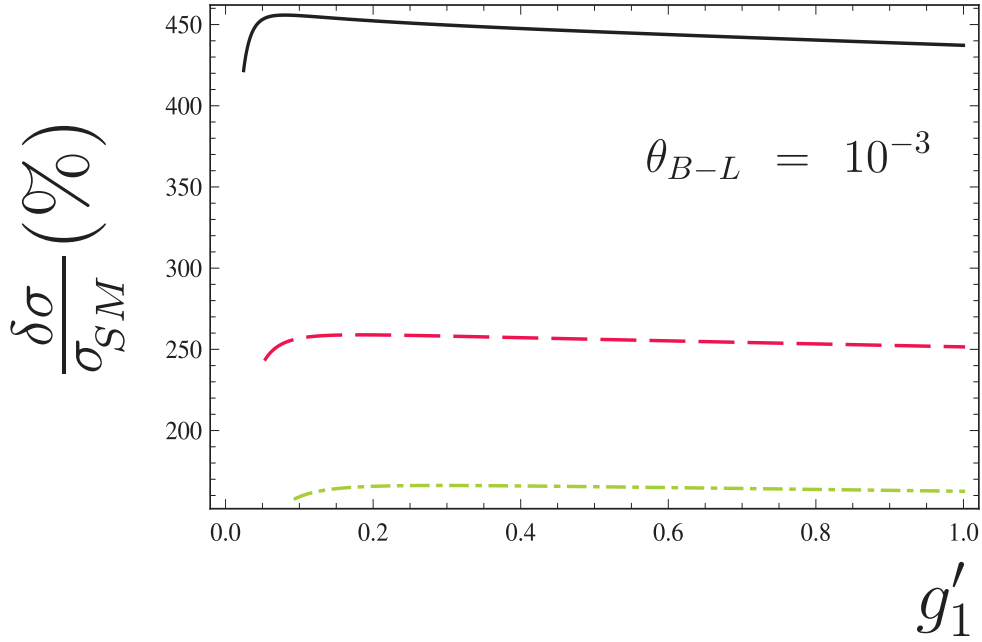


FIG. 6: The relative correction $\delta\sigma/\sigma_{SM}$ as a function of g'_1 . Starting from the top, the curves are for $M_{Z'} = 1500, 2000, 2500 \text{ GeV}$ and $\sqrt{s} = 1500, 2000, 2500 \text{ GeV}$, respectively.

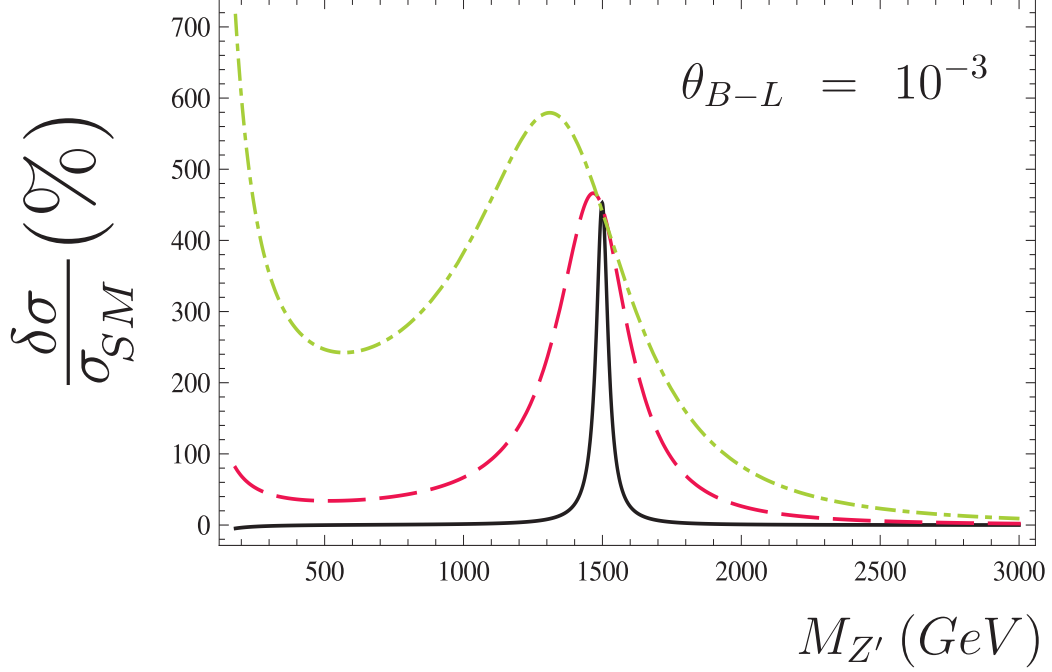


FIG. 7: The relative correction $\delta\sigma/\sigma_{SM}$ as a function of $M_{Z'}$. Starting from the bottom the curves are for $g'_1 = 0.2, 0.5, 0.8$ GeV and $\sqrt{s} = 1500$ GeV, respectively.

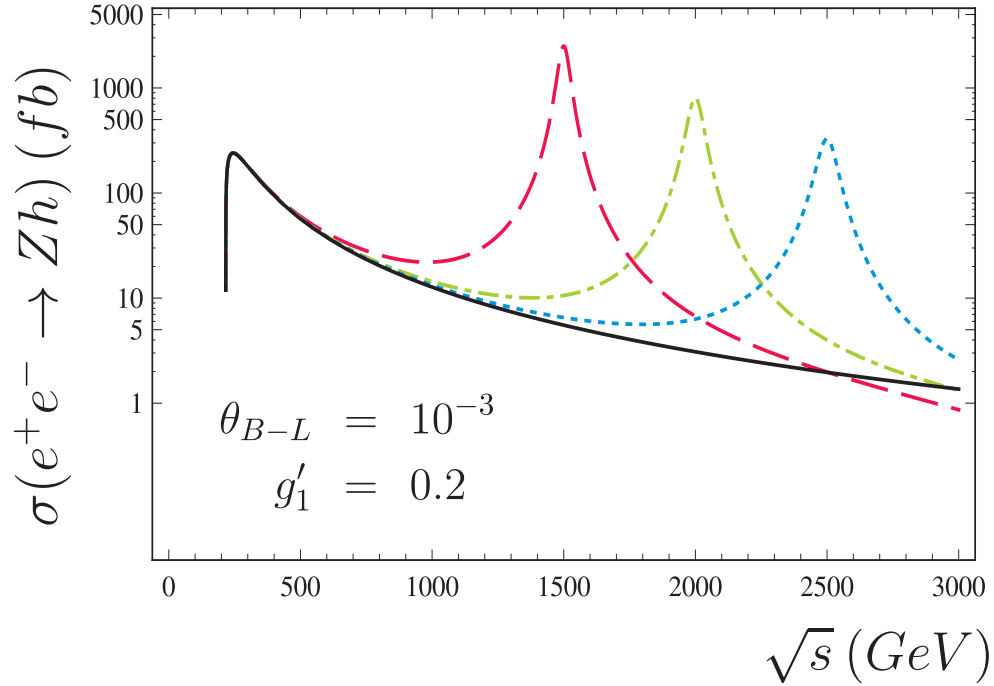


FIG. 8: The total cross sections of the production processes $e^+e^- \rightarrow Zh$ as a function of the collision energy. The curves are for SM (solid line) and $M_{Z'} = 1500, 2000, 2500$ GeV (dashed-line, dot-dashed line, dotted line). The resonance corresponds to the Z' new gauge boson.

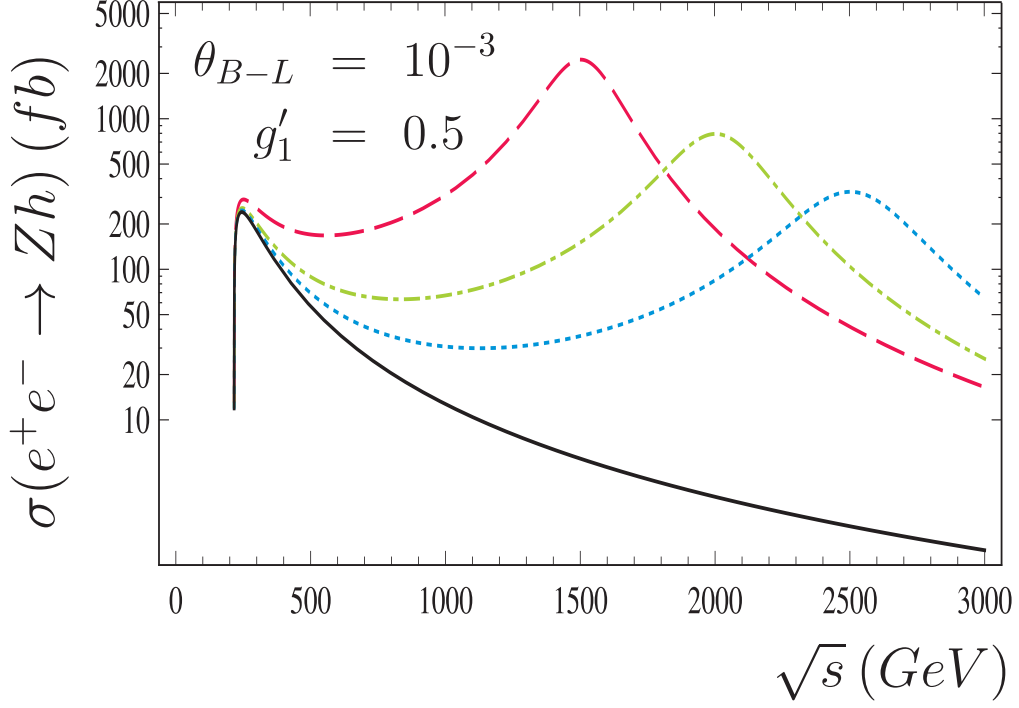


FIG. 9: The same as Fig. 8 but for $g'_1 = 0.5$.

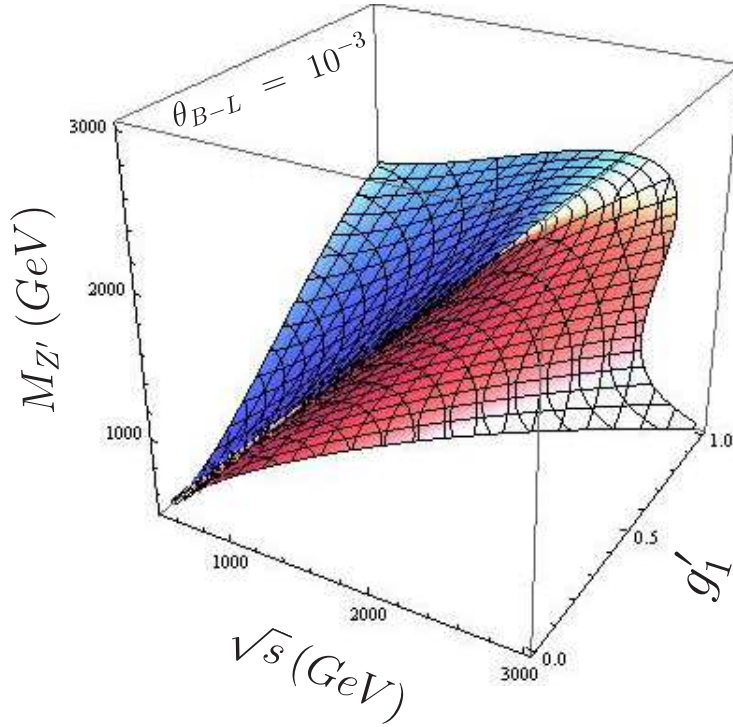


FIG. 10: Contour plot 3D for the total cross section $\sigma_{tot} = \sigma_{tot}(\sqrt{s}, M_{Z'}, g'_1)$ of the process $e^+e^- \rightarrow Zh$ for $M_h = 125 \text{ GeV}$ and $\theta_{B-L} = 10^{-3}$.

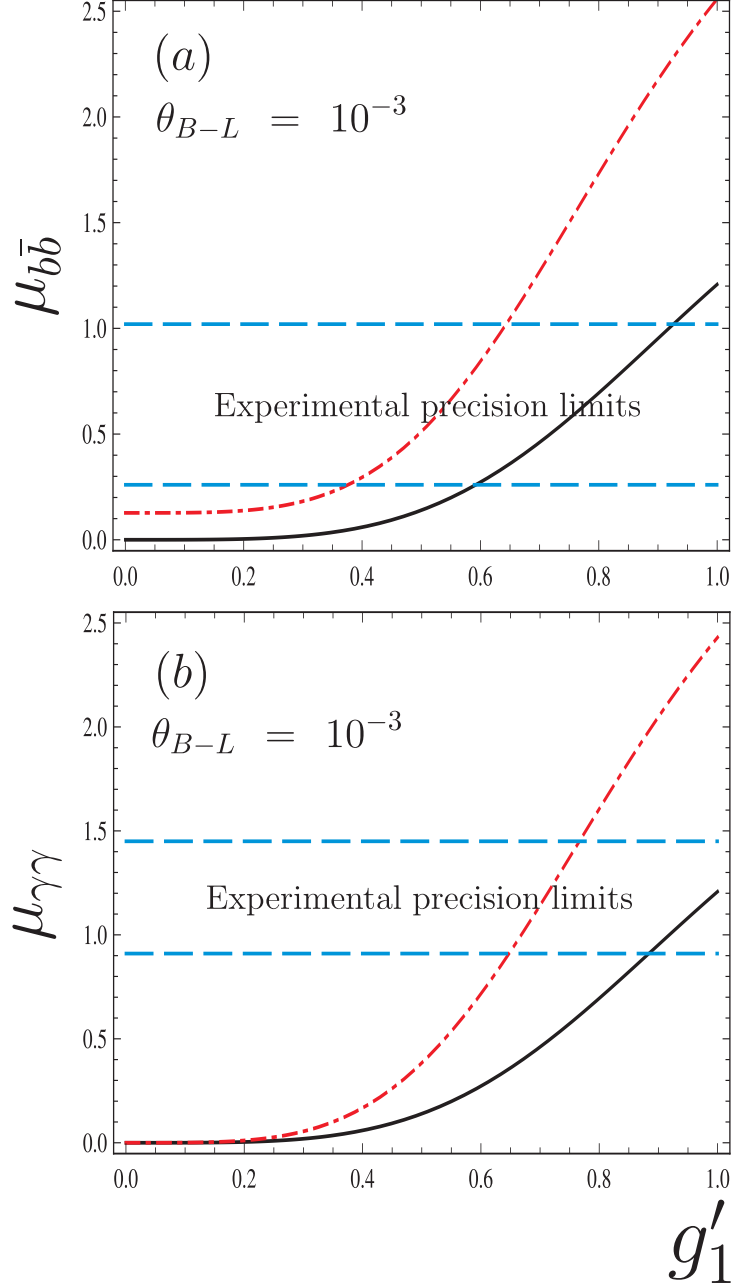


FIG. 11: Higgs signal strengths μ_i ($i = b\bar{b}, \gamma\gamma$) for the process $e^+e^- \rightarrow Zh$ as a function of g'_1 . The dashed lines represent the experimental precision limits and the solid and dot-dashed lines correspond to the $U(1)_{B-L}$ model with $M_h = 125 \text{ GeV}$ and $\sqrt{s} = 500, 1500 \text{ GeV}$, respectively.